

Random Walk Simulation for the Growth of Monolayer in Dip Pen Nanolithography

Hyojeong Kim, Soojung Ha, and Joonkyung Jang*

Department of Nanomaterials Engineering, Pusan National University, Miryang 627-706, Korea. *E-mail: jkjang@pusan.ac.kr
Received September 13, 2012, Accepted October 24, 2012

Using a simple random walk model, this study simulated the growth of a self-assembled monolayer (SAM) pattern generated by dip-pen nanolithography (DPN). In this model, the SAM pattern grew mainly *via* the serial pushing of molecules deposited from the tip. This study examined various SAM patterns, such as lines, crosses and letters, by changing the tip scan speed.

Key Words : Random walk, Self-assembled monolayer, Dip-pen nanolithography, Dendrite, Diffusion

Introduction

Dip-pen nanolithography (DPN) has emerged as a general tool for fabricating nanopatterns on a range of substrates, including metallic, insulating and semiconducting substrates.¹⁻³ In DPN, an atomic force microscope (AFM) tip functions as a source to continuously create nanodroplets of molecules that then spread to form a self-assembled monolayer (SAM) on a substrate. Molecular transport from the tip to the substrate is mediated by the water meniscus that naturally forms between the tip and substrate under ambient conditions.⁴⁻⁶

To assess the ultimate resolution and limitation of DPN, it is important to understand the fundamentals of DPN, particularly at the molecular level. Little is known about the molecular mechanisms and time scale of SAM growth in DPN. In this respect, theory and modeling have proven to be useful.^{4,7-10} Central to modeling DPN is how a nascent droplet (deposited from an AFM tip) spreads out to form a SAM afterward. Given that molecules are designed to chemisorb to a substrate, Jang *et al.*⁸ proposed a diffusion model of DPN assuming that the molecules are trapped irreversibly once they have reached the chemisorption sites on the substrate. Molecules can diffuse on top of other molecules. This model gives isotropic SAM patterns for a tip fixed in position but fails to reproduce the dendritic SAM patterns observed in DPN using dodecylamine¹¹ or polyethylene glycol¹² on mica. Molecular dynamics (MD) simulations⁷ showed that a SAM pattern grows mainly *via* a serial pushing mechanism (Figure 1(a)), in which a molecule in the upper layer (open circle in the second layer in the figure) pushes a molecule on the substrate out of its original position, and the molecule pushed out in turn pushes out another molecule nearby. Such a consecutive push propagates and reaches the periphery, after which the pushing stops. This serial pushing was taken to have a finite directional coherence length, N_d , which is defined as the number of consecutive pushing events in the same direction (see Figure 1(b)). By simply varying N_d , this model can reproduce a variety of SAM patterns, ranging from isotropic to dendritic patterns. The serial pushing model also captured the

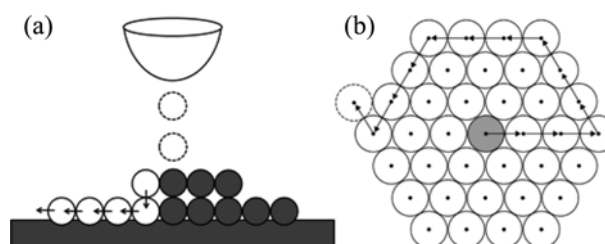


Figure 1. (a) Serial pushing model. A molecule (an open circle in the second layer) pushes the molecule below it (one of the open circles in the first layer), and the molecule pushed out in turn pushes its neighbor out of place. This pushing propagates (drawn as left arrows) toward the periphery of the monolayer until there is no molecule left to push out. (b) Schematic diagram of serial pushing events with the directional coherence length $N_d = 3$. The serial pushing changes its direction after every 3 consecutive pushing events.

essential features of the MD simulation.¹⁰ Previously, the serial pushing model was applied to cases where an AFM tip is fixed in position. On the other hand, the SAM patterns in DPN are generally made by moving the tip on a substrate. The outcome of DPN depends on the moving speed of the tip. In this study, various line-based SAM patterns were simulated to determine how DPN is affected by the tip scan speed and directional coherence length.

Details of Model and Simulation

Random walk simulations were performed using a three dimensional lattice and a discrete time step. A three dimensional lattice was constructed by vertically stacking replicas of a two dimensional trigonal lattice. The lattice spacing of the trigonal lattice, l , was identified as the distance between the nearest neighbor molecules in the SAM of octadecanethiol on a gold surface, $l = 0.5385$ nm.^{7,10} Every molecule lying above the monolayer on the substrate executes a random walk at every time step. If a random walk of such a molecule occurs directly toward a molecule below it, this random walk is taken to push the molecule below out of place. The molecule pushed out in turn pushes its neighbor out of place. This push-induced movement propagates

laterally toward the periphery until there are no molecules left to push out. This sequence of push-induced movements occurs without a time delay. Unlike the molecules in the upper layers, a molecule on the bare surface is allowed to move only if it is pushed by one of its nearest neighbors, above or beside it.

If a molecule initially pushes out its neighboring molecule, the subsequent $(N_d - 1)$ movements occur in the same direction as the initial pushing direction. The direction of the $(N_d + 1)^{\text{th}}$ molecular displacement becomes random, and the subsequent $(N_d - 1)$ movements are taken to occur in the same direction as the $(N_d + 1)^{\text{th}}$ displacement. This series of push-induced movement continues until it stops at the periphery (where there are no molecules left to push out). N_d was also assumed to follow the Poisson distribution,

$$P(N_d; \lambda) = \exp(-\lambda) \lambda^{N_d} (N_d!)^{-1}, \quad (1)$$

where the parameter λ is the average of N_d . A numerical random number generator was used to obtain $P(N_d; \lambda)$.

The time step of simulation Δt was set according to Jang *et al.*⁸ Δt and l must satisfy

$$4D\Delta t = l^2, \quad (2)$$

where D is the diffusion constant of the molecule. Here, estimating the value of D is difficult because D refers to the molecular diffusion on top of the other molecules (not the surface diffusion on a bare surface). Previously, D was estimated for eicosanethiol in the context of microcontact printing.¹³ Using this value $D = 7 \times 10^{-8} \text{ cm}^2 \text{ s}^{-1}$, $\Delta t = 10.4 \text{ ns}$.

In the present study, the tip scan speed v was reported in terms of a dimensionless value, v^* , which is defined as $v^* = v/(l/\Delta t)$. For a slow tip scan speed, $v^* < 1$, the tip moves by l for every $1/v^*$ time steps. If the displaced tip is not exactly at one of the lattice points, the tip position is taken to be at the lattice point closest to the tip position. Three tip scan speeds were considered, $v^* = 0.25, 0.5$, and 1 . Using the Δt value above, the actual tip scan speed v varies as 13, 26 and 52 mm/s. These scan speeds are comparable to the typical tip scan speeds used in the AFM experiments (several mm/s).^{14,15}

Another parameter needed for the present simulation is the dripping rate of molecules from the tip, n . Here, the dripping rate is reported in terms of a reduced rate, $n^* = n\Delta t$, which represents the number of molecules dropped per simulation time step. Throughout this study, n^* was fixed to 5. Previously, the dripping rate n was estimated experimentally to be $n = 4.2 \times 10^5 \text{ s}^{-1}$ for octadecanethiol molecules on a gold (111) surface.⁸ By using the present Δt , this value corresponds to $n^* = 4.368 \times 10^{-3}$. Therefore, the present simulation considers a relatively higher flux of molecules from the tip compared to the experiment.

Results and Discussion

The mechanism for how the SAM patterns are affected by varying N_d of the serial pushing was first examined. Figure 2 shows cross patterns generated at a tip scan speed v^* of 0.25.

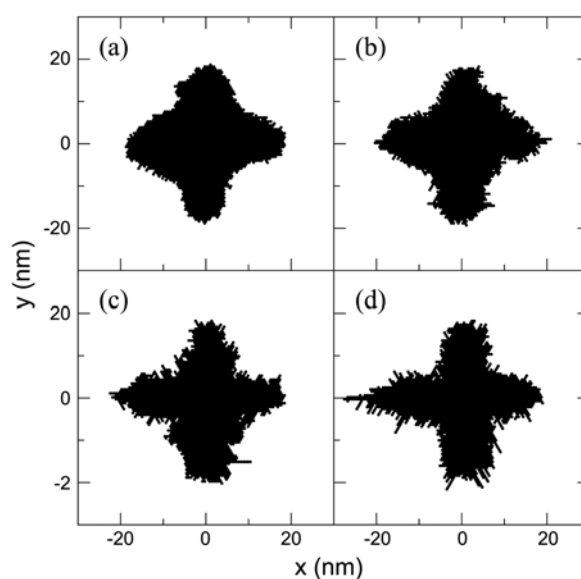


Figure 2. Cross SAM patterns generated by scanning a tip. The average N_d (λ in Eq. (1)) of serial pushing was varied as 1 (a), 10 (b), 20 (c), and 30 (d). The tip scan speed v^* and molecular dripping rate n^* were fixed to 0.25 and 5, respectively.

The vertical line is drawn first (from bottom to up) and the horizontal line is drawn next (from left to right). The periphery of the cross SAM pattern becomes more rugged as average N_d (λ in Eq. (1)) varies; 1 (a), 10 (b), 20 (c), and 30 (d). Compared to the case where the tip is fixed in position, the effects of changing N_d are small. A dendritic pattern with self-replicating branches was observed for high N_d values in the case of a fixed tip.¹⁰ On the other hand, no dendritic pattern was found for a moving tip.

The effects of tip scan speed on the SAM patterns were examined. The SAM line pattern was assessed by varying v^* ; 0.25 (a), 0.5 (b), and 1 (c) (Figure 3). The average N_d (λ) was fixed to 30 for all cases. As the tip scan rate increased, the width of the SAM line became narrower. Note that the

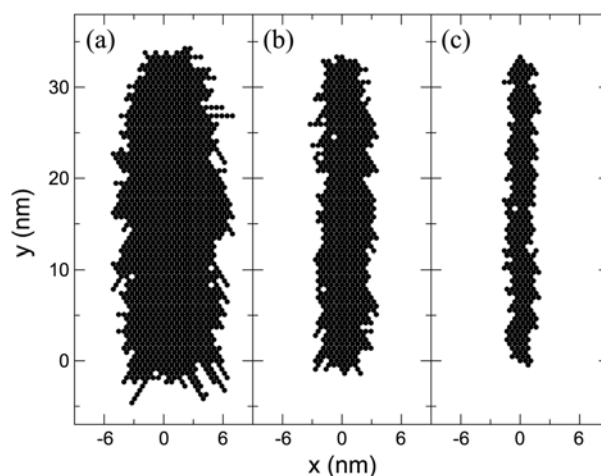


Figure 3. SAM lines patterned using the tip scan speeds v^* s of 0.25 (a), 0.5 (b), and 1 (c). The average directional coherence length (λ) and molecular dripping rate (n^*) were 30 and 5, respectively.

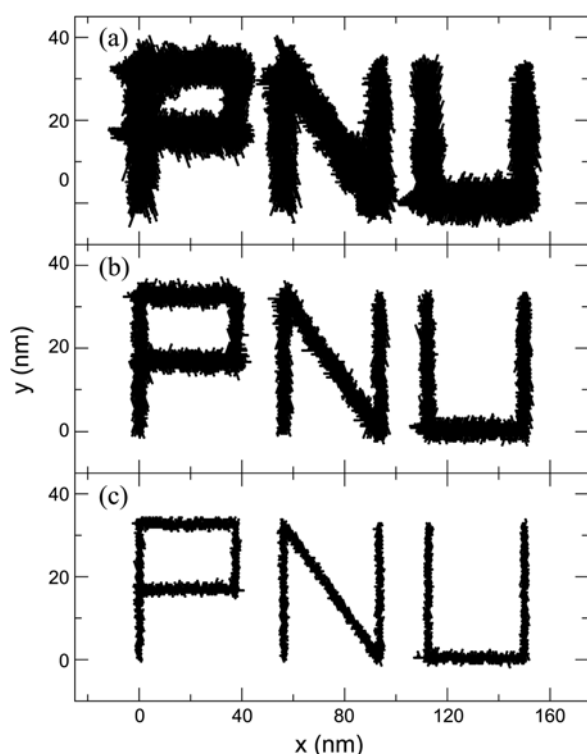


Figure 4. Letters generated using various tip scan speeds. v^* was varied, 0.25 (a), 0.5 (b), and 1 (c). The average directional coherence length (λ) and molecular dripping rate (n^*) are 30 and 5, respectively.

SAM line pattern becomes smoother in its periphery as the tip scan rate is increased, even though the same average N_d value was used for all cases in Figure 3.

Finally, the SAM letters made of lines were examined (Figure 4). As in the case of a SAM line, the letters became narrower and less rugged as the tip scan speed was increased. In these letter patterns, extra broadening was observed at the crossing points of the two lines.

In the context of the DPN experiments, these results suggest that an AFM tip should be scanned as fast as possible to achieve a SAM pattern with a narrow spatial resolution and with less rugged peripheries. On the other hand, a disconnected SAM pattern can occur if the scanning of a tip is too fast.

Conclusion

The growth of a SAM pattern in dip-pen nanolithography

was simulated using a simple random walk model. In this model, a SAM pattern grows primarily by the serial pushing of molecules initiated by molecules dropping from an AFM tip (source). This serial pushing was taken to have a finite length for its direction called the directional coherence length. To model the various SAM patterns made of lines, tip movement was implemented in the present simulation. For these line-based SAM patterns, the tip scan speed plays a major role in the outcome of DPN. As the tip scan speed increased, the SAM patterns became narrower and less rugged in their peripheries. The effect of the directional coherence length was relatively small compared to the case of a tip fixed in position.

Acknowledgments. This study was supported by National Research Foundation Grants funded by the Korean Government (MEST) (No. 2011-0027445 and No. 2011-0027696). J.J. wishes to thank the Korea Institute of Science and Technology Information for the use of the PLSI super-computing resources.

References

1. Piner, R. D.; Zhu, J.; Xu, F.; Hong, S.; Mirkin, C. A. *Science* **1999**, *283*, 661.
2. Mirkin, C. A. *ACS Nano* **2007**, *1*, 79.
3. Salaita, K.; Wang, Y.; Mirkin, C. A. *Nat. Nanotechnol.* **2007**, *2*, 145.
4. Kim, H.; Saha, L. C.; Saha, J. K.; Jang, J. *Scanning* **2010**, *32*, 2.
5. Rozhok, S.; Piner, R.; Mirkin, C. A. *J. Phys. Chem. B* **2002**, *107*, 751.
6. Giam, L. R.; Wang, Y.; Mirkin, C. A. *J. Phys. Chem. A* **2009**, *113*, 3779.
7. Heo, D. M.; Yang, M.; Kim, H.; Saha, L. C.; Jang, J. *J. Phys. Chem. C* **2009**, *113*, 13813.
8. Jang, J.; Hong, S.; Schatz, G. C.; Ratner, M. A. *J. Chem. Phys.* **2001**, *115*, 2721.
9. Kim, H.; Jang, J. *J. Phys. Chem. A* **2009**, *113*, 4313.
10. Kim, H.; Schatz, G. C.; Jang, J. *J. Phys. Chem. C* **2010**, *114*, 1922.
11. Manandhar, P.; Jang, J.; Schatz, G. C.; Ratner, M. A.; Hong, S. *Phys. Rev. Lett.* **2003**, *90*, 115505.
12. Rivas-Cardona, J. A.; Banerjee, D. *J. Micro/Nanolith. MEMS MOEMS* **2007**, *6*, 033004.
13. Delamarche, E.; Schmid, H.; Bietsch, A.; Larsen, N. B.; Rothuizen, H.; Michel, B.; Biebuyck, H. *J. Phys. Chem. B* **1998**, *102*, 3324.
14. Tzeng, S. D.; Lin, K. J.; Hu, J. C.; Chen, L. J.; Gwo, S. *Adv. Mater.* **2006**, *18*, 1147.
15. Szoszkiewicz, R.; Okada, T.; Jones, S. C.; Li, T.-D.; King, W. P.; Marder, S. R.; Riedo, E. *Nano Lett.* **2007**, *7*, 1064.